Journal of Chemical Health Risks

www.jchr.org

JCHR (2026) 16(1), 749-764 | ISSN:2251-6727

Integrated Computational and *In-Vitro* Approach Elucidates Multitarget Molecular Mechanisms Responsible for the Wound-Healing Activity of *Careya Arborea* Roxb.

Abhijit S. Salokhe[1], Archana S. Patil[1*], Sachin Gudasi[2], Ravikiran Kanbargi[1], Shailendra Sanjay Suryawanshi[3]

[1]Department of Pharmaceutics, KLE College of Pharmacy, Belagavi, KLE Academy of Higher Education and Research, Belagavi-591124, Karnataka, India.

[2]Department of Pharmacognosy, KLE College of Pharmacy, Belagavi, KLE Academy of Higher Education and Research, Belagavi-591124, Karnataka, India.

[3]Department of Pharmaceutical Analysis, KLE College of Pharmacy, Belagavi, KLE Academy of Higher Education and Research, Belagavi-591124, Karnataka, India.

Corresponding Author*

Dr. Archana S. Patil, Associate Professor, Department of Pharmaceutics, KLE College of Pharmacy, Belagavi, KLE Academy of Higher Education and Research, Belagavi-591124, Karnataka, India.

(Received: 25 November 2025 Revised: 27 December 2025 Accepted: 11 January 2026)

KEYWORDS

Careya arborea Roxb, Wound healing, Network pharmacology, Molecular docking, Systems pharmacology.

ABSTRACT:

Introduction: Careya arborea Roxb. is a medicinal plant widely employed in traditional systems of medicine for the treatment of wounds and inflammatory conditions. Despite its long-standing ethnopharmacological use, comprehensive scientific validation that integrates pharmacognostic standardization, phytochemical profiling, biological evaluation, and systems-level mechanistic understanding remains limited.

Objective: This study aimed to systematically investigate the wound-healing potential of C. arborea Roxb. bark using an integrated experimental and in silico approach to elucidate its phytochemical composition, biological efficacy, and underlying molecular mechanisms.

Methods: The bark of C. arborea Roxb. was collected, authenticated, shade-dried, and subjected to Soxhlet extraction using methanol. Pharmacognostic evaluation, including macroscopic, microscopic, and ash value analyses, was conducted to establish the identity, purity, and quality of the crude drug. Preliminary phytochemical screening was performed using standard qualitative assays. Network pharmacology analysis was applied to identify bioactive phytoconstituents and their putative wound-healing targets, followed by protein–protein interaction analysis, Gene Ontology, and KEGG pathway enrichment. Molecular docking studies were carried out against TNF-α, IL-6, and COX-2. In vitro anti-inflammatory activity was evaluated using protein denaturation and membrane stabilization assays, while antioxidant potential was assessed by the DPPH radical scavenging method.

Results: The bark extract exhibited a diverse phytochemical profile, including flavonoids, phenolics, tannins, saponins, alkaloids, triterpenoids, and glycosides. Network and enrichment analyses revealed a multitarget mechanism involving inflammatory, oxidative stress, angiogenic, and metabolic pathways. Molecular docking demonstrated strong binding affinities of key phytoconstituents toward inflammatory targets, and in vitro assays confirmed significant, concentration-dependent anti-inflammatory and antioxidant activities.

Conclusion: Overall, the findings provide compelling scientific evidence supporting the wound-healing potential of C. arborea Roxb. bark as a multitarget therapeutic candidate.

Journal of Chemical Health Risks

www.jchr.org

JCHR (2026) 16(1), 749-764 | ISSN:2251-6727

1. Introduction

Wound healing is a very coordinated and dynamic biological process involving overlapping phases of hemostasis, inflammation, proliferation, and remodeling, eventually allowing restoration of integrity of the tissue [1]. Disruption of any of these phases, particularly sustained inflammation, oxidative stress, impaired angiogenesis, and metabolic dysregulation, may result in delayed wound healing or chronic non-healing wounds, as commonly seen in diabetic and inflammatory conditions [2,3]. The wound-care therapies currently being used, such as antibiotics, anti-inflammatories, and growth factors, suffer mainly from the disadvantages of side-effects, high cost, and insufficient efficacy [4]. Therefore, these days, increasing research interest is being generated in plant-based therapeutics that offer multitarget synergistic mechanisms with a superior safety profile.

Careya arborea Roxb. family Lecythidaceae, commonly known as wild guava, is one of the recognized medicinal plants in traditional Indian medicine. Parts of the plant, especially the bark, were used traditionally for wound healing, ulceration, inflammation, and skin infection treatments [5]. Ethnopharmacological reports attribute mentioned therapeutic efficacy to the diverse bioactive phytoconstituents: flavonoids, phenolic acids, tannins, triterpenoids, saponins, and glycosides. These classes of compounds have been reported to exert antioxidant, anti-inflammatory, antimicrobial, and tissue-regenerative activities, all necessary for the efficient healing of wounds. However, despite their traditional relevance, better scientific validation for the wound-healing potential of C. arborea bark [6].

Recent advances in systems pharmacology and network-based approaches have enabled comprehensive exploration of complex herbal medicines by integrating phytochemical profiles with molecular targets and biological pathways [7]. Network pharmacology provides a powerful framework to decipher the multitarget and multipathway actions of phytoconstituents, particularly in multifactorial conditions such as wound healing. In parallel, in silico techniques such as protein–protein interaction (PPI) analysis, Gene Ontology (GO), Kyoto Encyclopedia of Genes and Genomes (KEGG) pathway enrichment, and molecular docking offer mechanistic insights into compound–target interactions at the molecular level [8,9]. When complemented with experimental validation, these approaches allow a holistic understanding of plant-based therapeutics.

Cytokines, inflammatory mediators par excellence such as tumor necrosis factor-α (TNF-α) and interleukin-6 (IL-6), and upregulation of cyclooxygenase-2 (COX-2) contribute to prolonged inflammation, cellular apoptosis, and degradation of the extracellular matrix [10]. Concomitantly, elevated levels of reactive oxygen species (ROS) inhibited fibroblast migration, reduced angiogenesis, and diminished collagen synthesis. Thus, it would be of great value to have therapeutic agents capable of recuperating redox balance while modulating inflammatory mediators in the management of a wound. Phytoconstituents such as quercetin, isoquercetin, ellagic acid, gallic acid, and triterpenoids have been known to be present in C. arborea as these phytoconstituents have been shown to influence these signaling pathways of interest, thus providing a strong mechanistic basis for their wound-healing activity [11,12].

In this context, the present study aims to systematically investigate the wound-healing potential of *Careya arborea* Roxb. bark through an integrated experimental and computational approach. The study encompasses pharmacognostic evaluation, phytochemical screening, network pharmacology analysis, PPI network construction, GO and KEGG pathway enrichment, and molecular docking against key inflammatory targets (TNF-α, IL-6, and COX-2). Furthermore, the anti-inflammatory and antioxidant activities of the bark extract were experimentally validated using in vitro protein denaturation, membrane stabilization, and DPPH radical scavenging assays. By combining traditional knowledge with modern systems biology and experimental validation, this work provides a comprehensive mechanistic framework supporting the therapeutic potential of C. arborea bark as a multitarget, plant-based agent for wound healing.

2. Materials and Methods

Collection, Authentication, and Extraction of Drug

The bark of *Careya arborea* Roxb. was collected from south-eastern Karnataka during March–April,

Journal of Chemical Health Risks
www.jchr.org
JCHR (2026) 16(1), 749-764 | ISSN:2251-6727

corresponding to the appropriate harvesting season. A qualified taxonomist authenticated the plant material at a recognized herbarium/institution, and a voucher specimen was deposited for future reference. The collected bark was washed thoroughly with running water to remove adhering soil and extraneous matter, followed by shade drying at ambient temperature (25–30 °C) for 10–12 days until a constant weight was achieved. The dried bark was then coarsely powdered using a mechanical grinder and sieved. For extraction, the powdered bark was subjected to Soxhlet extraction using methanol as the solvent [13]. Approximately 100 g of powdered material was packed into a thimble and extracted with methanol for 6–8 hours until the siphon tube showed colourless solvent. The extract was filtered, concentrated under reduced pressure using a rotary evaporator, and stored in airtight containers at 4 °C until further analysis.

Macroscopical Studies

Macroscopical evaluation of the crude drug was carried out to establish its identity and purity based on gross morphological characteristics. The collected and authenticated plant material was examined visually and with the aid of a hand lens to record external features such as colour, shape, size, surface texture, margin, apex, and overall structural pattern. Organoleptic properties, including appearance and texture, were also assessed. These macroscopic parameters were documented and compared with standard pharmacognostic descriptions to confirm the authenticity of the drug and to detect the presence of any adulterants or foreign matter [14].

Determination of Ash value

Ash value determination of the powdered, air-dried bark of *Careya arborea* Roxb. was carried out in accordance with standard pharmacopoeial methods to evaluate the presence of inorganic matter and to assess the purity and quality of the crude drug [15]. For total ash determination, approximately 2 g of the coarsely powdered sample was accurately weighed and incinerated in a silica crucible in a muffle furnace maintained at 450 °C until the material became carbon-free. The crucible was then cooled in a desiccator and weighed, and the total ash percentage was calculated with reference to the air-dried sample. To determine water-soluble ash, the total ash obtained was transferred to a beaker containing 25 mL of distilled water, boiled gently for 5 minutes, and filtered through filter paper. The insoluble residue was washed twice with warm water, ignited, cooled, and weighed. The weight of the insoluble matter was subtracted from the total ash to obtain the water-soluble ash, which was expressed as a percentage of the air-dried material. For acid-insoluble ash determination, the total ash was boiled with 25 mL of 2 M hydrochloric acid, filtered through ashless filter paper, and the residue was thoroughly washed with hot water. The filter paper along with the residue was ignited in a muffle furnace at 450 °C, cooled, and weighed. The acid-insoluble ash percentage was calculated to estimate the siliceous matter, including sand and earthy contaminants, and the results were recorded as quality control parameters [16, 17].

Phytochemical Screening

Preliminary phytochemical screening of the methanolic extract of *Careya arborea* Roxb. bark was carried out to qualitatively identify the presence of major classes of secondary metabolites using standard phytochemical procedures. The extract was subjected to specific chemical tests for the detection of alkaloids (Mayer's, Wagner's, and Dragendorff's tests), quinones (Bornträger's test), and carbohydrates (Molisch's, Benedict's, and Fehling's tests). Cardiac glycosides were identified using Keller–Killiani and Legal's tests [18]. The presence of flavonoids was assessed by alkaline reagent and lead acetate tests, while saponins were detected by the froth formation test. Triterpenoids and sterols were evaluated using Liebermann–Burchard and Salkowski reactions. Phenolic compounds and tannins were identified using ferric chloride and gelatin tests. Fatty acids were detected by spot and copper sulfate tests. All reactions were observed for characteristic color changes or precipitate formation. The results were recorded as present or absent, providing qualitative insight into the phytochemical composition of the bark extract [19].

Mining of phytoconstituents and proteins involved in Wound healing

The phytochemical profile of *Careya arborea* Roxb. was compiled based on an extensive review of published literature. Information on the identified phytoconstituents, including their chemical identities

Journal of Chemical Health Risks
www.jchr.org
JCHR (2026) 16(1), 749-764 | ISSN:2251-6727

and classifications, was systematically retrieved from the PubChem database. For each compound, canonical SMILES notations and PubChem Compound Identifiers (CIDs) were obtained and curated into a comprehensive dataset. To ensure data reliability and accuracy, duplicate phytoconstituents were carefully screened and removed during database construction. Putative molecular targets of the identified phytochemicals were predicted by submitting their SMILES representations to the DigiPred platform. Concurrently, wound healing–associated target genes were collected from the GeneCards database [20]. The predicted targets of the active phytoconstituents were then compared with disease-related genes to identify common targets. The overlapping targets between the phytochemical-associated genes and wound healing–related genes were determined using the Venny 2.1.0 tool. These intersecting targets were considered the most relevant molecular targets mediating the wound-healing potential of C. arborea Roxb. bark extract.

In-silico Studies

Building a component-disease-target-pathway network

Cytoscape version 3.7.1 was employed to construct and visualize the integrated "compound–disease–target–pathway" interaction network. The curated interaction data were imported into Cytoscape to enable systematic visualization and topological analysis of the network, facilitating the identification of key protein targets modulated by the phytoconstituents of *Careya arborea* Roxb. in the context of wound healing. The network was developed by linking active phytochemical constituents with their predicted molecular targets and associated wound healing pathways. Within the network, nodes represent phytocompounds, disease entities, target proteins, and signaling pathways, whereas edges denote the interactions among these components. Network visualization and screening were performed to evaluate the relative importance of nodes based on their connectivity, thereby highlighting potential hub targets and critical pathways involved in the wound-healing activity of *C. arborea* Roxb. [21].

Gene Ontology (GO) and Kyoto encyclopaedia of Genes and Genomes (KEGG) enrichment analysis

Gene Ontology (GO) and Kyoto Encyclopedia of Genes and Genomes (KEGG) enrichment analyses were conducted using an established online bioinformatics platform to elucidate the functional relevance of the identified target genes. GO enrichment analysis was performed across three categories: biological process (BP), molecular function (MF), and cellular component (CC). For each category, the top ten significantly enriched terms were identified based on P-value ranking. In parallel, KEGG pathway enrichment analysis was carried out to annotate the signaling pathways associated with the target genes. Pathways relevant to wound healing were subsequently filtered and selected for further interpretation, providing mechanistic insight into the biological processes and molecular pathways underlying the therapeutic potential of the phytoconstituents [22].

Molecular docking studies

Molecular docking studies were carried out to elucidate the binding orientation and interaction profiles of the selected phytochemical inhibitors within the active sites of the target proteins using the Schrödinger Glide module in Extra Precision (XP) mode. The XP docking protocol employs an advanced scoring function combined with extensive conformational sampling to minimize false-positive predictions and accurately rank ligand poses. Key noncovalent interactions, including hydrogen bonding, hydrophobic contacts, and π–π stacking interactions, were evaluated, with energetic penalties incorporated into the scoring function to ensure realistic pose discrimination. Phytocompound structures were generated using Maestro, and ligand preparation was performed through the LigPrep module of the Schrödinger suite. Energy minimization was conducted using the Optimized Potentials for Liquid Simulations (OPLS4) force field, and torsional flexibility was introduced to enhance binding complementarity. Crystal structures of TNF-α (PDB ID: 2AZ5), IL-6 (PDB ID: 1ALU), and COX-2 (PDB ID: 5KIR) were retrieved from the Protein Data Bank for in silico analysis. Protein structures were prepared using the Protein Preparation Wizard, where bond orders were assigned, missing hydrogen atoms were added, protonation states were optimized at physiological pH

Journal of Chemical Health Risks
www.jchr.org
JCHR (2026) 16(1), 749-764 | ISSN:2251-6727

(7.0 ± 0.2), and the structures were energy-minimized using the OPLS4 force field. Receptor grids were generated based on the co-crystallized ligands to accurately define the active binding sites, providing a robust framework for docking simulations [23,24].

***In vitro* Anti-inflammatory Activity**

Inhibition of Egg Albumin Denaturation

The anti-inflammatory potential of CAR was assessed using the protein denaturation method. In this assay, reaction mixtures were prepared in test tubes containing 0.2 mL of fresh hen's egg albumin, 2.8 mL of phosphate buffer (pH 6.4), and 2 mL of different concentrations of LM-AgNPs, LMLE, or the standard drug diclofenac sodium(n=3). The mixtures were initially incubated at room temperature for 15 min, followed by heating at 70 °C in a water bath for 5 min to induce protein denaturation. After heating, the samples were allowed to cool under running tap water. The absorbance of each sample was then measured at 660 nm using a UV-visible spectrophotometer [25], with phosphate buffer used as the blank. The percentage inhibition of egg albumin denaturation was calculated using the following equation:

Inhibition of denaturation (%) = [(Abs control – Abs sample)/Abs control] × 100

where Abs control is the absorbance of control solution; and Abs sample denotes the absorbance of sample.

Membrane Stabilisation Assay

Fresh blood samples were collected from a healthy volunteer, and erythrocyte suspensions were prepared according to standard procedures [42]. For each test, a total reaction volume of 2 mL was used, consisting of 1 mL of a 10% RBC suspension and 1 mL of test solution containing varying concentrations of CAR for the evaluation of heat-induced hemolysis inhibition. Aspirin was employed as the standard drug for comparison. The reaction mixtures were incubated in a water bath at 56 °C for 30 min with gentle mixing by periodic inversion. Following incubation, the samples were centrifuged at 2500 rpm at 37 °C. The tubes were then cooled under running water, and the supernatant was carefully collected. Absorbance of the supernatant was measured at 560 nm using a UV–visible spectrophotometer, with phosphate buffer serving as the blank [26].

Antioxidant Assay

The antioxidant activity of the methanolic extract of *Careya arborea* Roxb. was evaluated using the 2,2-diphenyl-1-picrylhydrazyl (DPPH) free radical scavenging assay. A freshly prepared DPPH solution (0.1 mM) in methanol was used for the analysis. Various concentrations of the plant extract (10–100 µg/mL) were prepared in methanol, and 1 mL of each concentration was mixed with an equal volume of DPPH solution. The reaction mixtures were incubated in the dark at room temperature for 30 minutes to allow complete reaction. Absorbance was measured at 517 nm using a UV–visible spectrophotometer. Ascorbic acid was used as the reference standard. The percentage of DPPH radical scavenging activity was calculated, and IC_{50} values were determined from the concentration–inhibition curves [27].

3. Result and discussion

Collection, Authentication and Plant Extraction

The bark of *Careya arborea* Roxb. was collected from Jamboti, south-west of Belagavi, Karnataka, and taxonomically identified by Dr. Ajit Lingayat (Shri B. M. K. Ayurveda Mahavidyalaya, KAHER, Belagavi). Soxhlet extraction of the powdered bark using methanol resulted in efficient recovery of bioactive constituents, yielding a dark brown, semi-solid extract with a percentage yield of approximately 12.8% w/w. Methanol, owing to its high polarity, effectively solubilized a broad spectrum of phytochemicals, including phenolics, flavonoids, tannins, and glycosides, which are associated with the therapeutic potential of the bark. Exhaustive extraction was confirmed by the appearance of colorless solvent in the siphon tube, indicating complete leaching of extractable components. Concentration under reduced pressure aided in preserving thermolabile constituents and minimizing solvent degradation. The resulting extract demonstrated good storage stability at 4 °C, with no observable precipitation or microbial growth during the study period.

Journal of Chemical Health Risks
www.jchr.org
JCHR (2026) 16(1), 749-764 | ISSN:2251-6727

Figure 1. (a) *Careya arborea* Roxb. plant (b)Bark

Microscopic Evaluation of Bark

Microscopic examination of the bark was performed using a photomicrographic system (Kyowa-Getner, Model 11UP) equipped with Bio-Plus-55 image analysis software. Transverse sections and powdered bark samples were prepared and examined using appropriate staining reagents to elucidate diagnostic histological features. Macroscopically, the bark was thick, rough, and dark grey in color, exhibiting shallow fissures with exfoliation in narrow flakes. It was odorless and characterized by a distinctly astringent taste. The transverse section revealed well-defined anatomical regions comprising cork, cortex, and secondary phloem. The cork consisted of 8–16 layers of thick-walled, rectangular cells with a blackish-brown appearance. The cortex was extensive and composed predominantly of parenchymatous cells that were rectangular to polygonal in shape. Numerous lignified fibers with very thick walls were observed; these fibers were elongated, slender, and prominently distributed, serving as key diagnostic features of the bark.

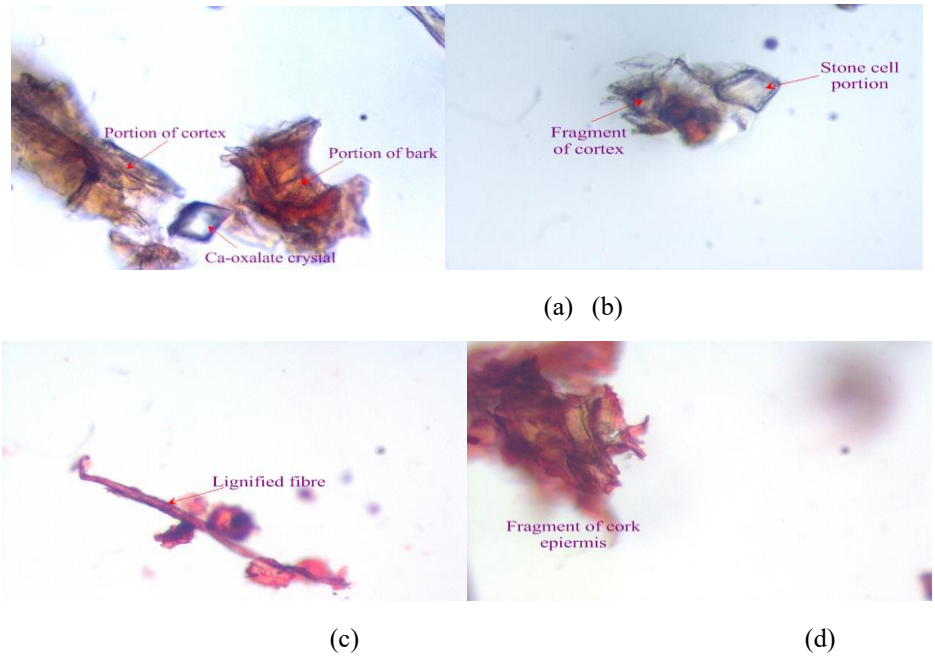

Figure 2. Microscopical characteristics of powdered bark of *Careya arborea* (a) Ca-Oxalate crystal, Portion cork & cortex (b) Fragment of cortex & stone cell (c) Lignified fibre (d) Fragment of cork epidermis

Ash Value Analysis

The ash values of the powdered bark of *Careya arborea* Roxb. are presented in Table 1. The total ash content was found to be **7.6 ± 0.62%**, indicating the overall amount of inorganic matter present in the crude drug. The **water-soluble ash value (3.55 ± 0.26%)** reflects the proportion of water-soluble inorganic salts, while the **acid-insoluble ash value (1.25 ± 0.35%)** represents the siliceous matter, such as sand and earthy

Journal of Chemical Health Risks
www.jchr.org
JCHR (2026) 16(1), 749-764 | ISSN:2251-6727

contaminants. The relatively low acid-insoluble ash content suggests minimal contamination with extraneous inorganic materials. Collectively, these ash values comply with acceptable pharmacognostic limits and serve as reliable quality control parameters for assessing the purity and authenticity of *Careya arborea* Roxb. bark.

Phytochemical testing

Preliminary phytochemical screening of the Soxhlet-extracted plant material revealed the presence of a wide range of bioactive secondary metabolites, as summarized in Table 1. The methanolic extract tested positive for cardiac glycosides, anthraquinone glycosides, saponins, flavonoids, coumarin glycosides, tannins, phenolic compounds, alkaloids, steroids, and triterpenoids, indicating the effectiveness of Soxhlet extraction in isolating both polar and moderately non-polar constituents. The absence of carbohydrates, as indicated by a negative Benedict's test, suggests minimal interference from simple sugars in the extract. The presence of flavonoids and phenolic compounds highlights the antioxidant and anti-inflammatory potential of the extract, while saponins and tannins are associated with antimicrobial and wound-healing activities. Alkaloids and cardiac glycosides contribute additional pharmacological relevance. Overall, the results demonstrate that Soxhlet extraction using methanol yields a phytochemically rich extract suitable for further formulation development and biological evaluation.

Table 1: Results of preliminary phytochemical screening.

Sr. No.	Phytoconstituents	Chemical tests	Leaf extract
1	Carbohydrates	Benedict's test	-
2	Cardiac Glycosides	Baljet's Test	+
3	Anthraquinone Glycosides	Borntrager's Test	+
		Modified Borntrager's Test	-
4	Saponin	Foam Test	+
	Glycosides		
5	Flavonoides	Alkaline reagent Test	+
6	Comarin glycosides	Ferric Chloride Test	+
7	Tannins & Phenolic	Ferric Chloride Test	+
8	Alkaloides	Dragendroff's Test	+
		Wager's Test	+
9	Steroids & Triterpenoids	Salkowski's test	+

Network construction and analysis *C. arborea* Roxb. Bark wound healing

Network pharmacology analysis was employed to elucidate the pharmacological mechanisms of *Careya arborea* Roxb. bark in wound healing by systematically evaluating compound–target interactions and their topological significance. The constructed network highlighted key bioactive constituents and molecular targets based on degree, neighborhood connectivity, and eccentricity parameters, reflecting their regulatory importance within the system. Among the identified phytoconstituents, isoquercetin (degree = 22), quercetin (15), casearborin A (15), ellagic acid (14), and betulin (12) exhibited high connectivity, suggesting their central roles in modulating multiple wound-healing–related targets. Notably, isoquercetin demonstrated the highest degree, elevated neighborhood connectivity (8), and minimal eccentricity (1), indicating its strong influence across the network and its capacity to act as a core multitarget regulator. These topological features suggest that isoquercetin may exert pleiotropic effects by simultaneously regulating inflammation, oxidative stress, angiogenesis, and metabolic dysregulation associated with diabetic wounds. Target-centric analysis identified PTPN1 as a key hub protein with extensive interactions. PTPN1 was connected to several high-degree compounds, including isoquercetin, quercetin, casearborin A, ellagic acid, betulin, barringtogenol C, barringtogenol D, and taraxerol acetate. Given the role of PTPN1 in insulin resistance and impaired healing, its modulation by multiple phytoconstituents supports a synergistic mechanism of

Journal of Chemical Health Risks
www.jchr.org
JCHR (2026) 16(1), 749-764 | ISSN:2251-6727

action. Collectively, the network architecture underscores the multitarget, multicomponent therapeutic potential of *C. arborea* bark in diabetic wound healing.

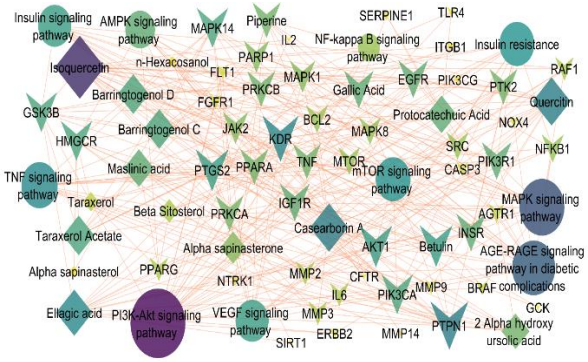

Figure 3. Network construction between Phytoconstituents, Targets and Pathways in kidney stone.

Gene Ontology (GO) enrichment analysis

The integrated Gene Ontology (GO) enrichment analysis encompassing biological processes, cellular components, and molecular functions delineates a comprehensive, systems-level framework underlying effective wound healing. At the biological process level, enrichment of responses to oxygen-containing compounds, chemical and endogenous stimuli, and organic substances highlights robust antioxidant and stress-adaptive mechanisms essential for restoring tissue homeostasis. Key regulators such as NOX4, NOS2, SIRT1, HIF1A, MAPKs, and NFKB1 coordinate redox balance, hypoxia adaptation, and inflammatory signaling, thereby supporting cell survival and angiogenesis within the wound microenvironment. Processes governing multicellular organismal regulation and biological quality reflect tight control of immune activation, vascular stability, and extracellular matrix (ECM) turnover. Matrix remodeling enzymes (MMP2, MMP9, SERPINE1) enable cell migration and re-epithelialization, while PIK3CA–AKT–mTOR and EGFR signaling promotes fibroblast and keratinocyte proliferation. Metabolic reprogramming, emphasized by lipid response pathways mediated via PPARs, INSR, and AKT1, ensures adequate energy supply during tissue repair.

At the cellular component level, significant localization of proteins to the cell periphery, plasma membrane, membrane rafts, and receptor complexes underscores the importance of membrane-associated sensing and signal initiation. Receptors and adhesion molecules such as EGFR, INSR, KDR, ITGB1, and TLR4 translate extracellular cues into intracellular responses that govern migration, proliferation, and inflammation. Enrichment of vesicles, cytoplasmic vesicles, and the endomembrane system reflects active protein trafficking, secretion, and recycling of cytokines, growth factors, and proteases. Localization to the extracellular region further supports ECM remodeling, immune cell recruitment, and inflammatory resolution.

At the molecular function level, dominant protein binding and enzyme binding activities indicate dense protein–protein interaction networks critical for coordinated signaling. Enriched catalytic and kinase activities, including MAPKs, PI3K, AKT, mTOR, and MMPs, drive phosphorylation-dependent signaling, angiogenesis, and matrix remodeling. Receptor binding, ion binding, and identical protein binding enhance signaling fidelity, enzymatic stability, and receptor dimerization. Collectively, these GO terms define an integrated molecular and cellular landscape that enables controlled inflammation, angiogenesis, metabolic adaptation, and efficient wound closure.

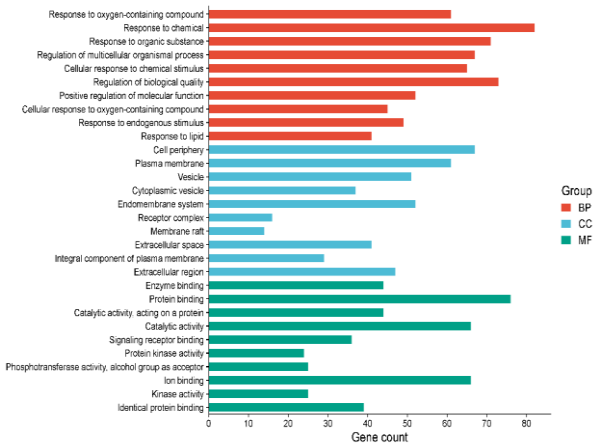

Figure 4. Gene ontology enrichment analysis of *C. arborea* Roxb.

KEGG pathway enrichment analysis

The KEGG pathway enrichment analysis highlights a coordinated, multitarget regulatory network underlying wound healing, particularly in metabolically compromised conditions such as diabetes. The AGE–

Journal of Chemical Health Risks
www.jchr.org
JCHR (2026) 16(1), 749-764 | ISSN:2251-6727

RAGE signaling pathway in diabetic complications, which shows the highest enrichment, is central to chronic wound pathology. Excessive AGE–RAGE activation promotes oxidative stress (NOX4), inflammatory signaling (NF-κB, TNF, IL-6), apoptosis (CASP3), and extracellular matrix degradation (MMPs). Modulation of this pathway alleviates persistent inflammation and restores tissue repair dynamics.

The PI3K–Akt signaling pathway acts as a core pro-survival and pro-regenerative axis in wound healing. Activation of PI3K, AKT1, and downstream mTOR enhances keratinocyte and fibroblast proliferation, promotes cell migration, inhibits apoptosis, and stimulates angiogenesis. Closely associated mTOR and AMPK signaling pathways regulate cellular energy homeostasis and protein synthesis, ensuring adequate metabolic support for granulation tissue formation and re-epithelialization. The MAPK signaling pathway contributes to wound repair by regulating cellular proliferation, differentiation, and stress responses. MAPKs (ERK, JNK, and p38) integrate growth factor and cytokine signals, thereby coordinating inflammatory resolution and tissue remodeling. Similarly, the TNF and NF-κB signaling pathways are crucial for the early inflammatory phase of wound healing. Controlled suppression of excessive TNF-α and NF-κB activity limits prolonged inflammation, reduces apoptosis, and prevents delayed healing. Angiogenesis is predominantly regulated by the VEGF signaling pathway, which promotes endothelial cell proliferation, migration, and neovascularization key processes for oxygen and nutrient delivery to the wound site. Finally, insulin resistance and insulin signaling pathways emphasize the restoration of glucose uptake and metabolic balance, which is critical for effective wound closure in diabetic conditions. Collectively, these interconnected pathways underscore a systems-level mechanism by which anti-inflammatory, antioxidant, pro-angiogenic, and metabolic regulatory effects synergistically accelerate wound healing.

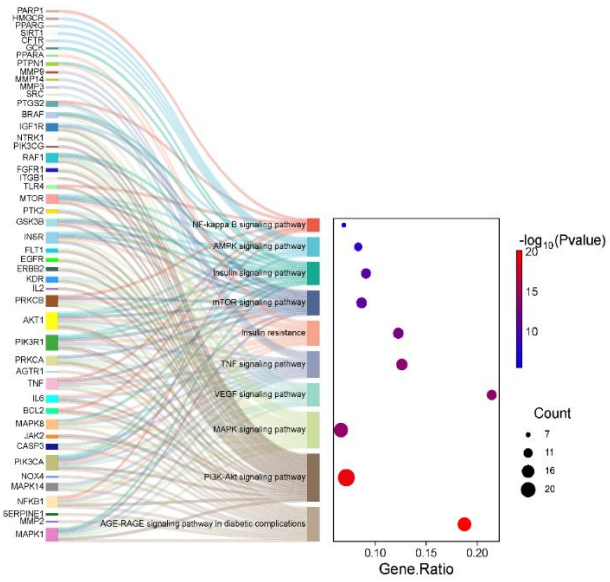

Figure 5. KEGG pathway analysis of *C. arborea* Roxb.

Molecular Docking study

The selected phytocompounds were subjected to molecular docking analysis to elucidate their preferred binding orientations and interaction patterns within the active sites of the selected target proteins, and the corresponding docking outcomes are summarized in Table 3. All ligand–protein complexes were rigorously evaluated based on their binding energies (expressed in kcal/mol) and detailed interaction profiles, including hydrogen bonding, hydrophobic contacts, and electrostatic interactions, which collectively contribute to the stability and specificity of ligand binding.

Docking analysis against tumour necrosis factor-α (TNF-α; PDB ID: 2AZ5) demonstrated that gallic acid exhibited a favourable binding affinity, with a docking score of −5.449 kcal/mol. Gallic acid formed stable hydrogen bond interactions with the TYR151 residue and an additional salt bridge interaction with LYS27, suggesting a strong and well-anchored binding mode within the TNF-α active site. Ellagic acid also showed appreciable binding, achieving a docking score of −4.945 kcal/mol, primarily stabilized through hydrogen bonding with TYR151 (Fig. 6). The relatively low (more negative) docking scores and consistent interaction patterns observed for these compounds indicate energetically favourable complex formation and support their potential role as TNF-α inhibitors.

Journal of Chemical Health Risks
www.jchr.org
JCHR (2026) 16(1), 749-764 | ISSN:2251-6727

Similarly, molecular docking against interleukin-6 (IL-6; PDB ID: 1ALU) revealed effective binding of phenolic phytoconstituents within the cytokine's active region. Gallic acid exhibited a docking score of −4.170 kcal/mol and formed multiple hydrogen bond interactions with key residues, notably LYS27 and ASP26, which are critical for ligand stabilization within the IL-6 binding pocket. Quercetin showed comparable binding affinity, with a docking score of −4.177 kcal/mol, and established an extensive hydrogen-bonding network involving GLU30, ASP26, ARG30, and LEU181 (Fig. 7). The favourable docking energies and the involvement of functionally relevant residues suggest that these compounds may effectively interfere with IL-6–mediated inflammatory signalling.

Notably, docking studies targeting cyclooxygenase-2 (COX-2; PDB ID: 5KIR) revealed particularly strong interactions for flavonoid-based phytochemicals. Isoquercetin exhibited a markedly high binding affinity, with a docking score of −11.993 kcal/mol, and formed multiple hydrogen bonds with essential active-site residues, including SER530, ARG513, MET522, and ARG120. Ellagic acid also demonstrated strong binding to COX-2, with a docking score of −9.772 kcal/mol and comparable interaction features (Fig. 8). The substantially high docking scores observed for these compounds underscore their strong binding propensity and suggest potent inhibitory potential against COX-2–mediated inflammatory pathways.

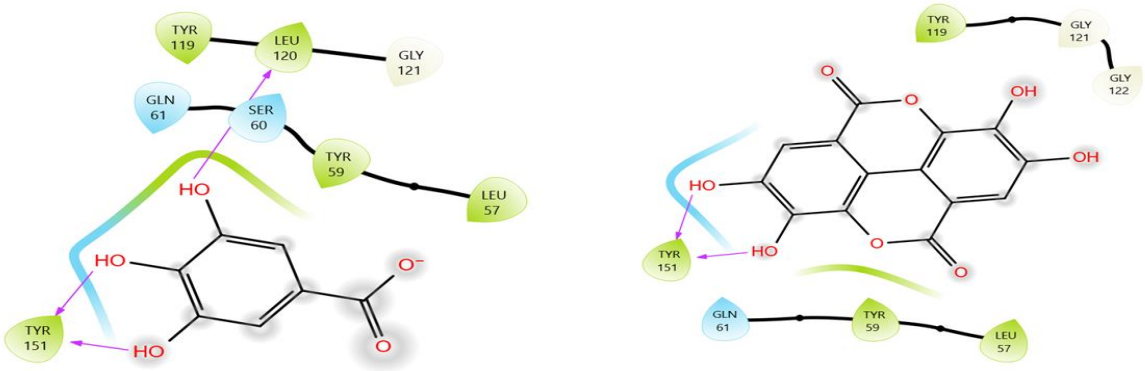

Figure 6. Binding Affinity of phytoconstituent with PDB ID: 2AZ5

Table 2. Binding affinity of Phytocompounds

Title	Docking Score	Glide Energy	Hydrogen Bond Interactions
2AZ5 - prepared			
Gallic Acid	-5.449	-20.200	LEU120, TYR151
Ellagic acid	-4.945	-27.837	TYR151
Isoquercetin	-4.879	-31.071	TYR151, GLN61, TYR59, LEU120
Quercitin	-4.551	-24.559	TYR59
Protocatechuic Acid	-4.479	-18.295	TYR151
Maslinic acid	-4.058	-24.107	GLN149, TYR151
Barringtogenol C	-3.193	-20.822	TYR151, GLY121
Barringtogenol D	-3.193	-20.822	TYR151, GLY121
2 Alpha hydroxy ursolic acid	-2.736	-24.079	GLN149

Journal of Chemical Health Risks
www.jchr.org
JCHR (2026) 16(1), 749-764 | ISSN:2251-6727

Taraxerol Acetate	-2.448	-28.146	-
Alpha-sapinasterol	-2.375	-17.944	-
Beta Sitosterol	-2.285	-22.077	-
Betulin	-2.198	-22.610	TYR151, GLY121
Alpha sapinasterone	-2.184	-19.355	-
Piperine	-1.243	-26.502	-
Casearborin A	2.011	-28.924	LYS98

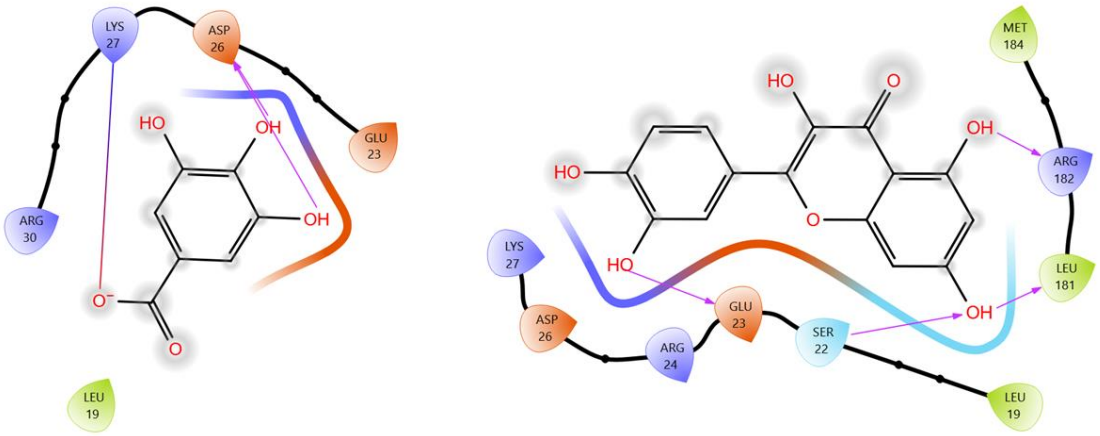

Figure 7. Binding Affinity of phytoconstituent with PDB ID: 1ALU

Table 3. Binding affinity of Phytocompounds

Title	**Docking Score**	**Glide Energy**	**Hydrogen Bond Interactions**
1ALU - prepared			
Gallic Acid	-4.170	-21.450	LYS27, ASP26
Quercitin	-4.166	-28.478	GLU30, ASP26, ARG30, LEU181
Barringtogenol C	-4.040	-26.408	LYS27, ARG182
Barringtogenol D	-4.040	-26.408	ARG182, LYS27
Isoquercetin	-4.019	-40.833	GLU30, ASP26, ARG30, LEU181
Protocatechuic Acid	-3.560	-20.576	LYS27, ASP26
Maslinic acid	-1.873	-22.821	ASP26, LYS27
2 Alpha hydroxy ursolic acid	-1.773	-22.799	ARG24
Alpha sapinasterone	-1.657	-19.248	-
Ellagic acid	-1.369	-20.067	LYS27, GLU23

Journal of Chemical Health Risks
www.jchr.org
JCHR (2026) 16(1), 749-764 | ISSN:2251-6727

Beta Sitosterol	-0.741	-19.868	-
Alpha sapinasterol	-0.735	-15.832	-
Taraxerol Acetate	-0.622	-22.262	ARG30
Taraxerol	-0.539	-17.406	GLN28
Betulin	-0.218	-15.373	GLN28, LEU19
Piperine	0.163	-20.946	-
n-Hexacosanol	0.731	-30.251	ARG24
Casearborin A	12.756	-30.366	LYS27, ARG30

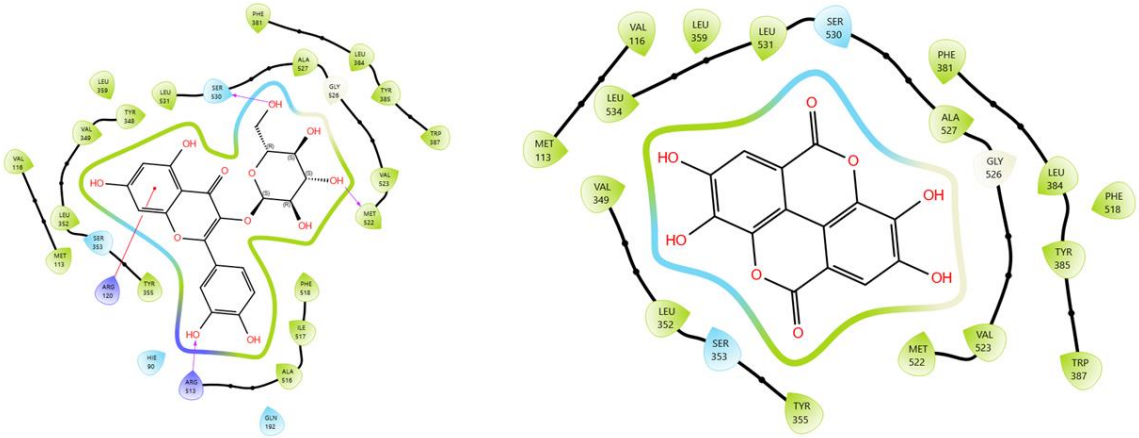

Figure 8. Binding Affinity of phytoconstituent with PDB ID: 5KIR

Table 4. Binding affinity of Phytocompounds

Title	**Docking Score**	**Glide Energy**	**Hydrogen Bond Interactions**
5KIR - prepared			
Isoquercetin	-11.993	-14.456	SER530, ARG513, MET522, ARG120
Ellagic acid	-9.772	-29.858	-
Quercitin	-8.702	-40.026	PHE518, SER530
Gallic Acid	-7.632	-28.800	SER30, MET522
Protocatechuic Acid	-6.506	-23.616	MET522
Piperine	-6.109	-23.836	-

Journal of Chemical Health Risks
www.jchr.org
JCHR (2026) 16(1), 749-764 | ISSN:2251-6727

In vitro Anti-inflammatory Activity

Protein Denaturation Assay

Protein denaturation involves the loss of a protein's native three-dimensional structure due to external stress conditions such as heat, pH variation, or chemical exposure, resulting in loss of biological activity. Denatured proteins may expose hidden antigenic determinants that are recognized by the immune system as non-self, thereby initiating and sustaining inflammatory responses. This phenomenon is closely associated with inflammatory disorders such as arthritis and other chronic inflammatory conditions. Consequently, inhibition of protein denaturation is widely accepted as a reliable in vitro indicator of anti-inflammatory potential of therapeutic agents. The anti-inflammatory activity of the test sample (CAR) was evaluated using the protein denaturation assay and compared with the standard drug aspirin. The results demonstrated a clear concentration-dependent inhibition of protein denaturation for both CAR and aspirin over the concentration range of 200–1000 µg/ml. At 200 µg/ml, CAR exhibited 30 % inhibition, while aspirin showed 32 % inhibition. At 400 µg/ml, the inhibition increased to 38 % for CAR and 43 % for aspirin. At 600 µg/ml, both CAR and aspirin showed equal inhibition of 52 %, indicating comparable protective effects against protein denaturation. Further enhancement was observed at higher concentrations, where CAR showed 72 % and 90 % inhibition at 800 and 1000 µg/ml, respectively, while aspirin exhibited 75 % and 92 % inhibition at the same concentrations. The results suggest that CAR effectively stabilizes proteins against denaturation in a dose-dependent manner and exhibits anti-inflammatory activity comparable to aspirin, supporting its potential role as a promising anti-inflammatory agent.

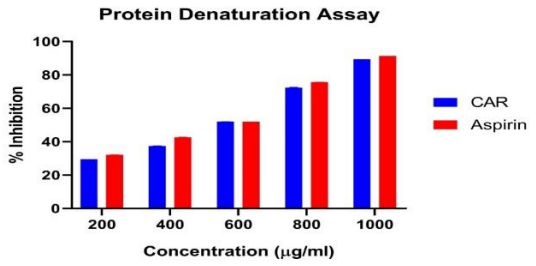

Figure 9. Protein Denature Assay of *Careya arborea* Roxb. Extract

Membrane Stabilisation Assay

Membrane stabilization is an important mechanism in the management of inflammation, as the stabilization of lysosomal and erythrocyte membranes prevents the release of inflammatory mediators such as proteases, phospholipases, and pro-inflammatory enzymes at the site of inflammation. During inflammatory conditions, destabilization of cellular and lysosomal membranes leads to increased membrane permeability and subsequent hemolysis, thereby aggravating tissue damage and inflammatory responses. Therefore, the ability of a test compound to inhibit hemolysis of erythrocyte membranes in vitro is considered a reliable indicator of its anti-inflammatory potential, as erythrocyte membranes closely resemble lysosomal membranes in composition and structural integrity.

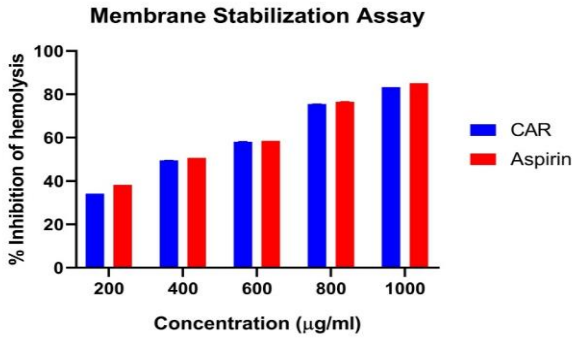

Figure 10. Membrane stabilization assay of *Careya arborea* Roxb. Extract

The membrane stabilization activity of the test sample (CAR) was evaluated and compared with the standard anti-inflammatory drug aspirin at concentrations ranging from 200 to 1000 µg/ml. As shown in the figure, both CAR and aspirin exhibited a concentration-dependent inhibition of hemolysis. At 200 µg/ml, CAR showed 34% inhibition of hemolysis, while aspirin exhibited 38% inhibition. With increasing concentration to 400 µg/ml, the inhibitory effect increased to 50% for CAR and 52% for aspirin. At 600 µg/ml, *Careya arborea* Roxb. demonstrated 58% inhibition, comparable to aspirin (59%). A marked increase in membrane stabilization was observed at higher concentrations, where CAR exhibited 75% and 84% inhibition at 800 and 1000 µg/ml, respectively, while aspirin showed 77% and 86% inhibition at the same concentrations. These results indicate that *Careya*

Journal of Chemical Health Risks
www.jchr.org
JCHR (2026) 16(1), 749-764 | ISSN:2251-6727

arborea Roxb. effectively stabilizes erythrocyte membranes in a dose-dependent manner and displays membrane protective activity comparable to aspirin. The observed membrane stabilization suggests that CAR may exert its anti-inflammatory effect by preventing lysosomal membrane rupture and subsequent release of inflammatory mediators, thereby supporting its therapeutic potential as an anti-inflammatory agent.

Antioxidant Assay

The antioxidant potential of the *Careya arborea* Roxb. extract was evaluated using the DPPH free radical scavenging assay, which measures the ability of antioxidants to reduce the stable DPPH radical from its purple-colored radical form to a yellow-colored non-radical form. Ascorbic acid, employed as the reference standard, exhibited pronounced antioxidant activity, with an IC_{50} value of 14.84 µg/mL and a maximum percentage inhibition of 82.45% at 25 µg/mL, reflecting its high free radical scavenging efficiency. The methanolic extract of *Careya arborea* Roxb. showed moderate antioxidant activity, with an IC_{50} value of 57.17 µg/mL and a maximum inhibition of 60.99% at 50 µg/mL. This activity can be attributed to the presence of phenolic compounds and flavonoids, which are capable of neutralizing free radicals through electron donation, hydrogen atom transfer, and radical quenching mechanisms, thereby contributing to the antioxidant potential of the extract.

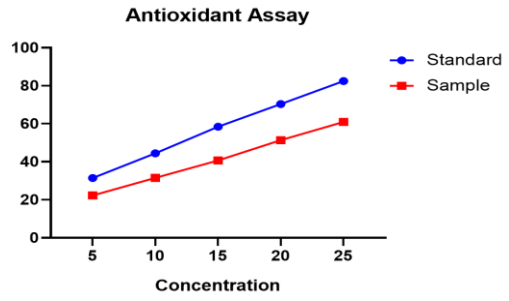

Figure 11. Antioxidant assay of *Careya arborea* Roxb. Extract

4.Conclusion

The present investigation provides an integrated pharmacognostic, phytochemical, biological, and computational validation of the wound-healing potential of *Careya arborea* Roxb. bark. Standardized collection, authentication, and extraction ensured the reproducibility and quality of the plant material, while macroscopic, microscopic, and ash value analyses confirmed its identity and purity in accordance with pharmacopoeial standards. The methanolic bark extract was found to be rich in diverse secondary metabolites, notably flavonoids, phenolics, tannins, saponins, alkaloids, and triterpenoids, which are well recognized for their roles in tissue repair, inflammation control, and oxidative stress modulation. Network pharmacology and protein–protein interaction analyses revealed that the wound-healing activity of *C. arborea* is mediated through a multicomponent–multitarget mechanism, with key hub proteins and pathways regulating inflammation, angiogenesis, extracellular matrix remodeling, and metabolic homeostasis. GO and KEGG enrichment analyses further demonstrated the coordinated involvement of critical signaling cascades, including AGE–RAGE, PI3K–Akt, MAPK, TNF/NF-κB, VEGF, and insulin signaling pathways, which are essential for efficient wound repair, particularly under diabetic or inflammatory conditions. Molecular docking studies substantiated the strong binding affinity and inhibitory potential of major phytoconstituents against pivotal inflammatory mediators such as TNF-α, IL-6, and COX-2. In vitro anti-inflammatory, membrane stabilization, and antioxidant assays corroborated the computational findings, revealing dose-dependent activities comparable to standard drugs. Overall, this study highlights *C. arborea* Roxb. bark as a scientifically validated, multitarget wound-healing agent and supports its further development as a phytopharmaceutical or adjunct therapeutic for chronic and inflammatory wounds.

Conflicts of interest

The author has no conflicts of interest regarding this investigation.

References

1. Mamun AA, Shao C, Geng P, Wang S, Xiao J. Recent advances in molecular mechanisms of skin wound healing and its treatments. Frontiers in immunology. 2024 May 21;15:1395479. https://doi.org/10.3389/fimmu.2024.1395479
2. Wang Q, Liu C, An J, Liu J, Wang Y, Cai Y. Mechanisms of microbial infection and wound healing in diabetic foot ulcer: pathogenicity in the

inflammatory-proliferative phase, chronicity, and treatment strategies. Frontiers in Endocrinology. 2025 Oct 1;16:1657928. https://doi.org/10.3389/fendo.2025.1657928

3. Schilrreff P, Alexiev U. Chronic inflammation in non-healing skin wounds and promising natural bioactive compounds treatment. International journal of molecular sciences. 2022 Apr 28;23(9):4928. https://doi.org/10.3390/ijms23094928
4. Borges A, Calvo ML, Vaz JA, Calhelha RC. Enhancing Wound Healing: A Comprehensive Review of Sericin and Chelidonium majus L. as Potential Dressings. Materials. 2024 Aug 24;17(17):4199. https://doi.org/10.3390/ma17174199
5. Kaur MA, Yadav RA. Pharmacognostic, ethnopharmacological, phytochemical and pharmacological profile of wild Guava ie Careya arborea Roxb. Int J Curr Pharm Res. 2017;9(3):1-7.
6. Sewwandi PA, Kugaseelan S, Virajini MT, Samarakoon KW, Jayasooriya PT, Kuruppu AI. Exploring the Potential Antioxidant, Anti-Inflammatory, and Anticancer Properties of Careya arborea: A Promising Underutilized Source of Natural Therapeutics. Wild. 2025 Nov 11;2(4):44. https://doi.org/10.3390/wild2040044
7. Mukherjee PK, Banerjee S, Kar A. Molecular combination networks in medicinal plants: understanding synergy by network pharmacology in Indian traditional medicine. Phytochemistry reviews. 2021 Aug;20(4):693-703. https://doi.org/10.1007/s11101-020-09730-4
8. Leung EL, Cao ZW, Jiang ZH, Zhou H, Liu L. Network-based drug discovery by integrating systems biology and computational technologies. Briefings in bioinformatics. 2013 Jul 1;14(4):491-505. https://doi.org/10.1093/bib/bbs043
9. Bhat GR, Sethi I, Rah B, Kumar R, Afroze D. Innovative in silico approaches for characterization of genes and proteins. Frontiers in Genetics. 2022 May 18;13:865182. https://doi.org/10.3389/fgene.2022.865182
10. Laveti D, Kumar M, Hemalatha R, Sistla R, Gm Naidu V, Talla V, Verma V, Kaur N, Nagpal R. Anti-inflammatory treatments for chronic diseases: a review. Inflammation & Allergy-Drug Targets-Inflammation & Allergy). 2013 Oct 1;12(5):349-61. https://doi.org/10.2174/18715281113129990053
11. Riaz A, Ali S, Summer M, Noor S, Nazakat L, Aqsa, Sharjeel M. Exploring the underlying pharmacological, immunomodulatory, and anti-inflammatory mechanisms of phytochemicals against wounds: a molecular insight. Inflammopharmacology. 2024 Oct;32(5):2695-727. https://doi.org/10.1007/s10787-024-01545-5
12. Sultana A, Borgohain R, Rayaji A, Saha D, Das BK. Promising phytoconstituents in diabetes-related wounds: mechanistic insights and implications. Current Diabetes Reviews. 2025 Feb;21(2):E270224227477. https://doi.org/10.2174/0115733998279112240129074457
13. Alara OR, Abdurahman NH, Ukaegbu CI, Kabbashi NA. Extraction and characterization of bioactive compounds in Vernonia amygdalina leaf ethanolic extract comparing Soxhlet and microwave-assisted extraction techniques. Journal of Taibah University for Science. 2019 Dec 11;13(1):414-22. https://doi.org/10.1080/16583655.2019.1582460
14. Encarnação S, Serrano R, Almeida C, Silva O. Micromorphology and Chemical Studies on Anacardium occidentale L. Stem Bark as an Herbal Medicine. Plants. 2022 Dec 20;12(1):7. https://doi.org/10.3390/plants12010007
15. Ciarnoschi LD, de Oliveira LC, Simeone ML, dos Santos Panero F, dos Santos Panero P, Rodriguez AR, Alves Filho EG, Pereira MG, da Silva LM. Prediction of dry matter, carbon and ash contents and identification of Calycophyllum spruceanum (Benth) organs by Near-Infrared spectrophotometry. Microchemical Journal. 2022 Sep 1;180:107621. https://doi.org/10.1016/j.microc.2022.107621
16. Kipo SL, Ofori-Kwakye K, Kuntworbe N, Johnson R, Boakye-Gyasi ME, Osei YA, Owusu FA. Physicochemical and microbiological characteristics of stem bark exudate gum of Cordia millenii tree in conventional release tablets. The Scientific World Journal. 2023;2023(1):9118067. https://doi.org/10.1155/2023/9118067
17. Malengue A, Lourenço A, Patrício H, Costa RA, Quilhó T, Gominho J. Tropical mobola plum (Parinari Curatellifolia): a full characterization of

wood and bark within the scope of biorefineries. European Journal of Wood and Wood Products. 2024 Aug;82(4):1021-35. https://doi.org/10.1007/s00107-024-02074-2

18. Hassan Cheong ND, Zakaria LA, Yusof H. Qualitative Phytochemical Screening and Antibacterial Properties of Momordica charantia Methanolic Extract Against Selected Bacterial Strains. Malaysian Journal of Medicine & Health Sciences. 2022 Oct 5;18.
19. Rahman TU, Khan H, Liaqat W, Zeb MA. Phytochemical screening, green synthesis of gold nanoparticles, and antibacterial activity using seeds extract of Ricinus communis L. Microscopy Research and Technique. 2022 Jan;85(1):202-8. https://doi.org/10.1002/jemt.23896
20. Gudasi S, Gharge S, Koli R, Kagawad P. Exploring in-silico, in-vitro antioxidant, and cytotoxic potential of valerian wallichii by on cervical epithelial carcinoma (HeLa) cell lines. Chemistry & Biodiversity. 2024 Mar;21(3):e202302072. https://doi.org/10.1002/cbdv.202302072
21. Gudasi S, Gharge S, Koli R, Patil K. Antioxidant properties and cytotoxic effects of Oxalis corniculata on human Hepatocarcinoma (Hep-G2) cell line: an in vitro and in silico evaluation. Future Journal of Pharmaceutical Sciences. 2023 Mar 28;9(1):25. https://doi.org/10.1186/s43094-023-00476-2
22. Kavalapure RS, Alegaon SG, Gharge S, Ranade SD, Gudasi S, Venkatasubramanian U. Structure-guided development of Quinoline derivatives targeting kinesin spindle protein. Bioorganic & Medicinal Chemistry Letters. 2025 Sep 1;125:130278. https://doi.org/10.1016/j.bmcl.2025.130278
23. Gharge S, Alegaon SG, Jadhav S, Ranade SD, Kavalapure RS. Design, synthesis, characterization and Antidiabetic evaluation of 3, 5-substituted thiazolidinediones: Evidenced by network pharmacology, Molecular docking, dynamic simulation, in vitro and in vivo assessment. European Journal of Medicinal Chemistry Reports. 2024 Dec 1;12:100213. https://doi.org/10.1016/j.ejmcr.2024.100213
24. Ranade SD, Alegaon SG, Khatib NA, Gharge S, Kavalapure RS, Kumar BP. Design, synthesis, molecular dynamic simulation, DFT analysis, computational pharmacology and decoding the antidiabetic molecular mechanism of sulphonamide-thiazolidin-4-one hybrids. Journal of Molecular Structure. 2024 Sep 5;1311:138359. https://doi.org/10.1016/j.molstruc.2024.138359
25. Chaiya P, Senarat S, Phaechamud T, Narakornwit W. In vitro anti-inflammatory activity using thermally inhibiting protein denaturation of egg albumin and antimicrobial activities of some organic solvents. Materials Today: Proceedings. 2022 Jan 1;65:2290-5. https://doi.org/10.1016/j.matpr.2022.04.916
26. Sangeeta MK, Tejashree, Gunagambhire VM, Bhat MP, Nagaraja SK, Gunagambhire PV, Kumar RS, Mahalingam SM. In-vitro evaluation of Talaromyces islandicus mediated zinc oxide nanoparticles for antibacterial, anti-inflammatory, bio-pesticidal and seed growth promoting activities. Waste and Biomass Valorization. 2024 Mar;15(3):1901-15. https://doi.org/10.1007/s12649-023-02386-z
27. Venkataesan Kumari B, Mani R, Asokan BR, Balakrishnan K, Ramasamy A, Parthasarathi R, Kandasamy C, Govindaraj R, Vijayakumar N, Vijayakumar S. Green synthesised silver nanoparticles using Anoectochilus elatus leaf extract: Characterisation and evaluation of antioxidant, anti-inflammatory, antidiabetic, and antimicrobial activities. Journal of Composites Science. 2023 Nov 1;7(11):453. https://doi.org/10.3390/jcs7110453